Assessing Invariant Mining Techniques for Cloud-based Utility Computing Systems

Antonio Pecchia, *Member, IEEE,* Stefano Russo, *Senior Member, IEEE,* and Santonu Sarkar, *Member, IEEE*

Abstract—Likely system invariants model properties that hold in operating conditions of a computing system. Invariants may be mined offline from training datasets, or inferred during execution. Scientific work has shown that invariants' mining techniques support several activities, including capacity planning and detection of failures, anomalies and violations of Service Level Agreements. However their practical application by operation engineers is still a challenge. We aim to fill this gap through an empirical analysis of three major techniques for mining invariants in cloud-based utility computing systems: clustering, association rules, and decision list. The experiments use independent datasets from real-world systems: a Google cluster, whose traces are publicly available, and a Software-as-a-Service platform used by various companies worldwide. We assess the techniques in two invariants' applications, namely executions characterization and anomaly detection, using the metrics of coverage, recall and precision. A sensitivity analysis is performed. Experimental results allow inferring practical usage implications, showing that relatively few invariants characterize the majority of operating conditions, that precision and recall may drop significantly when trying to achieve a large coverage, and that techniques exhibit similar precision, though the supervised one a higher recall. Finally, we propose a general heuristic for selecting likely invariants from a dataset.

Index Terms—Invariants, Cloud, SaaS, Workload characterization, Anomaly detection.

1 Introduction

Dynamic invariants are properties of a program or a system expected or observed to hold during executions. Dynamic *program invariants* can be inferred from execution traces as *likely invariants* [1], a relaxed form modeling properties which hold during one or more executions, though not necessarily over all possible executions. Program likely invariants have been shown to support several software engineering activities [2] [3] [4] [5].

Likely system invariants [6] are attractive for modeling runtime behavior of data centers and cloud-based utility computing systems from a service operation viewpoint. They are *operational abstractions* of their dynamics.

Due to the size and complexity of such systems, it is very hard for human operators to detect application problems in real time. Especially transient or silent errors occur rarely - e.g. in case of overload, timing issues and exceptions - and often do not cause an immediately observable failure such as a crash or hang, hence are hard to detect. Typically, likely system invariants hold in normal operating conditions; as such, their violations are considered symptoms of execution malfunctions. By monitoring execution and checking for broken invariants, it is possible to automatically detect failures [7] and to request actions to the operations personnel (e.g. jobs re-execution).

Defining invariants is pretty natural for cluster computing or Software-as-a-Service (SaaS) platforms, and generally for systems performing batch work, providing services to applications often consisting of *jobs*, in turn comprising *tasks*. These systems include monitoring and logging facilities[1] collecting metrics - e.g., job/task completion time, resource usage and status codes - which can be used to establish invariants. Indeed, likely system invariants have been shown to be effective for modeling execution dynamics in a variety of service computing systems [8], and for supporting a range of operational activities, including capacity planning, detecting anomalous behaviors [9], silent failures [10], and violations of service level agreements [11].

While previous scientific work has shown that invariant mining techniques may be beneficial for the above goals, practitioners face several problems, including *(i)* how to select a proper technique for their analysis goals, *(ii)* how many invariants are needed, and *(iii)* what accuracy they can expect. We cope with the challenge of filling the gap between past studies and the concrete usage of likely system invariants by operations engineers of cloud-based utility computing systems. By empirically analyzing and comparing techniques to mine invariants, we contribute to gain quantitative insights into advantages and limits of such techniques, providing operation engineers with practical usage implications and a heuristic to select a set of invariants from a dataset.

The study focuses on three techniques: two unsupervised, namely *clustering* and *association rules*, and one supervised, *decision list*. They are applied to two independent datasets collected in real-world systems: a cluster operated by Google, whose traces from about 12,500 machines are publicly available, and a SaaS platform in use by various medium- to large-scale consumer packaged goods (CPG) companies worldwide. The datasets comprise 679,984 executions (correct and anomalous) of batch units of work, namely jobs and transactions.

We explore the use of the techniques for two typical applications of invariant-based analysis, namely *executions characteriza-*

- *A. Pecchia is with the Consorzio Interuniversitario Nazionale per l'Informatica (CINI), Via Cinthia, 80126, Napoli, Italy. E-mail: antonio.pecchia@consorzio-cini.it.*
- *S. Russo is with Dipartimento di Ingegneria Elettrica e Tecnologie dell'Informazione, Università di Napoli Federico II, Via Claudio 21, 80125 Napoli, Italy. E-mail: stefano.russo@unina.it.*
- *S. Sarkar is with the Birla Institute of Technology & Science, Pilani K K Birla Goa Campus, NH 17 B, Zuarinagar, Goa, India. E-mail: santonus@goa.bits-pilani.ac.in.*

Manuscript received July 30, 2016.

1. E.g., Nagios (www.nagios.org) and Ganglia (http://ganglia.info).

tion and *anomaly detection*. We assess them based on the widely used metrics coverage, precision and recall. A sensitivity analysis is performed to carefully explore the invariants returned by each technique under different settings of the mining algorithms.

The key findings of the study are:

- The considered techniques provide a valuable support for characterizing executions and detecting anomalies in an automated way. For the SaaS cloud platform in particular, using the mined invariants it was possible to provide a valuable result to the service operation team of the IT company, spotting true anomalies for a number of transactions out of the seven month's of operation data, which were indeed missing and went unnoticed.
- *A relatively small number of invariants hold in a majority of system executions*. For example, in the Google dataset less than 10 invariants cover more than the 80% of job executions (using *association rules* - Apriori algorithm). Using further invariants does not increase coverage significantly. No *few-fits-all* invariants can be practically mined to characterize all system executions. The coverage of the *correct* executions is roughly 80%-90% for both datasets.
- *Invariants are very sensitive to the coverage: small variations of the coverage impact significantly recall and precision*. For instance, the recall of *association rules* (Apriori algorithm) for the Google cluster drops from 0.54 to 0.33 when coverage increases from 68% to 77%; similarly, when the coverage of *clustering* (DBSCAN algorithm) raises from 87% to 92%, precision drops from 0.35 to 0.01 for SaaS. *There seems to be a sort of threshold phenomenon*: recall/precision are strongly bound to the coverage of the correct executions.
- *Precision is surprisingly similar across the techniques*; for example, its maximum value in this study is about 0.7 in the Google dataset.
- *As for recall, the decision list supervised technique outperforms the unsupervised clustering and association rules.*
- *In spite of the best coverage, association rules are not well suited for anomaly detection*; notwithstanding the smaller coverage, invariants mined by decision list achieve higher recall/precision for anomaly detection.
- *We propose a general heuristic for selecting a set of likely invariants from a dataset*.

The paper is structured as follows. Section 2 surveys related work. Section 3 introduces the datasets used for experiments. Section 4 presents the mining techniques. Section 5 describes the evaluation metrics. Section 6 compares the techniques with respect to typical applications of invariants, i.e., executions characterization and anomaly detection. Section 7 provides practical recommendations to practitioners and a heuristic to select invariants. Section 8 discusses threats to the validity of the study. Section 9 contains concluding remarks.

2 Related Work

Program invariants were introduced by Ernst et al., who presented techniques for inferring *likely invariants* from program execution traces [1]. Likely program invariants are a valuable support for several software engineering activities, including selection of test inputs [2], discovery of interface specifications [3], testing compatibility of COTS components [4], enforcement of relational database schema constraints [5].

System invariants have been shown by several authors to be effective for modeling system dynamics and for detecting anomalous behaviors. Jiang et al. [6] introduced the concept of *flow intensity* in transactional systems, whose behavior depends on user requests. They presented an approach for modeling the relationships between the flow intensities, and demonstrated experimentally that *flow intensity invariants* do exist for distributed transaction system. In [12] they used the technique for detecting faults like memory leaks, missing files and null calls.

Sharma et al. [8] described positive experiences in a variety of IT systems with the SIAT product built around the flow intensity mining algorithms, used 24x7 for detecting invariants and locating faults as well as for capacity planning; they reported that the violation detection can be performed in seconds, after a training in the order of minutes.

Lou et al. [9] discovered invariants from console logs of Hadoop and CloudDB, revealing constant linear characteristics of program work flows, used for detecting execution anomalies.

Miao et al. [10] described an approach for silent failure detection in wireless sensor networks by finding correlation patterns.

In [11] we have described a framework to discover dynamic invariants from application logs, and supporting the online detection of violations of Service Level Agreements in SaaS systems.

For all these applications, invariants were mined from various types of data sources, mainly with techniques based on *time series analysis*, possibly refined with graph-based techniques.

In their work on flow intensity invariants in transactional systems, Jiang et al. [6] mine time series in monitoring data using AutoRegressive models with eXogenous inputs (ARX) [13] to learn linear relationships between pairs of flow intensities (called *local invariants*). In the subsequent work [14] the computational complexity of the invariant search algorithm is overcome with two further algorithms which are approximate but more efficient.

The mining of flow intensity invariants suffers from the combinatorial explosion of the search space when applied to *global invariants*, i.e. to higher order correlations among system attributes. Hence, in [15] a Bayesian regression technique was proposed for global invariants: first a regression model is built, whose solution is such that only spatially correlated attributes have non-zero coefficients; then temporal dependencies of attributes are considered. The application to a wireless UMTS system shows that the technique achieves the detection rate 0.848; just a very rough estimate is provided of the false positive rate (as low as 0.08).

In their work on the SIAT tool [8], Sharma et al. discussed also two approaches to reduce noise in broken invariants so as to support faults localization in a distributed sensors system: a *spatial* approach exploiting a graph of the extracted invariants, and a *temporal* approach which marks an invariant as actually broken only if it is broken for three consecutive samples of a time series.

In the previous work [11] we too used an ARX model of time series from 9 months of log events of a SaaS platform. With respect to [8], we mined invariants with much higher goodness of fit using a Recursive Least Square algorithm adapted from [13], yielding a relatively small number of invariants whose violation is directly indicative of the fault location.

In [16] we discussed accuracy and completeness of invariant-based anomaly detection, showing that *(i)* a well tuned approach can reach good completeness at an accuracy in the range 50-74%; *(ii)* the sampling time can be set to find a tradeoff between the mining time and the violation detection time, respectively in the order of minutes and seconds, confirming what reported in [8].

As for the datasets used in this study, it is worth considering various analyses of the publicly available Google cluster dataset [17]. This is a trace log of one of Google cloud data centers; it contains data of jobs running on 12,500 servers for a period of 29 days, accounting for 25 millions submitted tasks.

Di et al. [18] used a K-means clustering algorithm to classify applications in an optimized number of sets based on task events and resource usage; they also found a correlation between task events and application types, with about 81.3% of fail events belonging to batch applications. Chen et al. used the dataset for analysis [19] and prediction [20] of job failures; Guan and Fu [21] identified anomalies through Principal Component Analysis of monitored system performance metrics. Rosà et al. [22] analyze unsuccessful tasks/jobs executions and propose Neural Networks-based prediction models. While these studies do not specifically address invariants, some of their results about workload characterization and failures identification are in line with the ones we present based on the three mining techniques.

In summary, the literature shows that invariants can be mined and used effectively for a wide range of computing systems - data centers, cloud systems, web hosting infrastructures, wireless networks and sensors-based distributed systems. We are not aware of any work comparing mining techniques on different datasets, so as to learn practical usage implications and general heuristics useful for practitioners. This is the goal of the present study.

3 DATASETS

3.1 Google cluster

We provide a short description of the dataset, whose details can be found in [17]. The workload consists of tasks, each running on a single machine. Every task belongs to one job; a job may have multiple tasks (e.g., mappers and reducers). There are six tables in the dataset: *Machine_events, Machine_attributes, Job_events, Task_events, Task_constraints* and the *Resource_Usage*. Every job and every machine is assigned a unique 64-bit identifier. Tasks are identified by means of the ID of their job and an index; most resource utilization measurements are normalized.

Machines are described by two tables. *Machine_events* reports addition, removal or update of a machine to the cluster, along with its CPU and memory capacity. *Machine_attribute* lists key-value pairs of attributes representing properties such as kernel version, clock speed, and presence of an external IP address. Attributes are integers if there is a small number of values for the attribute; obscured strings based on a technique proposed in [23], otherwise. The *Job_events* and *Task_events* tables describe jobs/tasks and their lifecycle. They indicate transitions between the states shown in Fig. 1. The *Task_constraints* table lists task

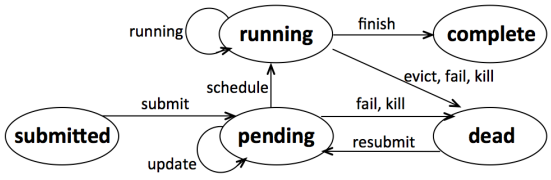

Fig. 1: State transitions of the jobs in the Google cluster dataset.

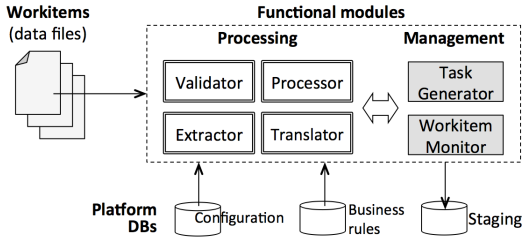

Fig. 2: High-level architecture of the SaaS platform.

placement constraints that restrict the machines onto which tasks can be scheduled. Usually all tasks in a job execute exactly the same binary with the same options and resource request. The *Resource_Usage* table reports resource usage of the tasks.

3.2 SaaS platform

The SaaS platform we consider provides cloud-based data processing and analysis capability to several consumer packaged good (CPG) companies. The platform accepts and transforms data files provided by customers through FTP servers or email attachments.

The data files, referred to as **workitems**, go trough **processing stages**, such as format validation, verification, data extraction and transformations. Once a data file is accepted by the SaaS platform, a **transaction** is started: the processing stages of a workitem are run in the context of the transaction. Based on the outcome of the latest processing stage, the transaction is either continued or aborted; it is completed if all the processing stages are accomplished successfully. At any time through all the elaboration, the status of a transaction can assume one out of four values, i.e., *in_process*, *user_error*, *exception*, and *processed*. *User_error* and *exception* denote the failure of the transaction.

A processing stage within a transaction can result in a success or a failure: if successful, the transaction moves to the next stage. Upon the failure of a stage *(i)* the platform generates an exception, *(ii)* the transaction is aborted, and *(iii)* the customer is notified about the problem for future resubmission or correction. Further details of the platform can be found in [11]; a reliability analysis of the operational failures is presented in [24].

Fig. 2 shows the high-level architecture of the SaaS platform. The *processing* modules implement the above-mentioned stages; *management* modules are responsible for handling the transactions workitems pertain to, and monitoring the progression of the stages. The platform relies on databases containing the *configuration* and *business rules* (e.g., management of customers and data files); the *staging* database maintains intermediate results/transformations of the workitems and internal audit logs containing execution informations and error events. Logs are stored as database tables. Applications and DBs server are based on VMWare ESX VMs running on Intel Xeon processors.

In this study we use the *Details Log* table. Each line (examples are shown by Table 1) lists details and outcome of a processing stage, such as the id of the workitem and start/end times. Important fields are *Stage* (the processing stage), *Status* (the outcome of the stage), and *Fail Reason* (a short textual description of the outcome). The log has been collected during operation from April to October 2012, covering a time frame of seven months.

TABLE 1: SaaS dataset: structure of the *Details* log.

Event	Workitem	Stage	START time	END time	Fail Reason	Status
4346482	308145	IT3	2012/05/02 01:57:54	2012/05/02 01:57:54	Corrupt_File	L1_REJ
4346810	309135	IT3_PVLD	2012/05/10 10:24:32	2012/05/10 10:25:03	Invalid_File	L1_REJ
4347484	309467	IT4_TRNF	2012/05/12 04:13:42	2012/05/12 04:13:45	System_Error	SE

4 Invariant Mining

A **workload unit** W (i.e., a *job* in the datacenter or a *processing stage of a transaction* in the SaaS platform) is abstracted by a set of N **attributes** $A_1, A_2, \ldots, A_N$. These attributes represent the computing resources used or parameters such as duration, priority and return codes, being collected during the execution of W. The attributes that characterize the execution of a workload unit assume a value in the Cartesian product $\{V_{A_1} \times V_{A_2} \cdots \times V_{A_N}\}$, where V_{A_j} denotes the set of the possible values of $A_j (1 \leq j \leq N)$. The values of the attributes are extracted from the input dataset to form an $M \times N$ **attributes matrix**, where M denotes the total workload units W_i ($1 \leq i \leq M$).

Fig. 3 shows the framework and steps that underlie invariant mining. Given the input monitoring data at a given time t_i, *(i)* **workload abstraction** infers the M workload units W_i and the values of the attributes for each W_i; *(ii)* **invariant mining** infers the set of recurring relationships among the values of the attributes from the data collected until t_i, i.e., *invariants* I_{t_i} in Fig. 3. At t_i==t_0 (where t_0 denotes the time of the first ever mining), the set of invariants available to operations engineers is I=I_{t_0}, which is mined from the data at t_0. Moreover, engineers will select a subset of invariants in I, i.e., *actionable invariants* in Fig. 3, that will be used for a specific application, e.g., anomaly detection.

Invariants might undergo reviews/changes upon feedback by operations engineers. From a *methodological* standpoint the framework encompasses the scenarios shown by Fig. 3: *(i)* **refinement** of the actionable invariants based on application results, field experience or domain knowledge (e.g., to fix a rule that runs in too many missed detections); *(ii)* entire **update** of I when new incoming data become available at t_i>t_0 and, for example, engineers deem the system has been subjected to major workload changes or hardware/software upgrades. In the latter case I is merged/replaced with the new set of invariants I_{t_i} found at t_i (*dotted box* in Fig. 3); new actionable invariants are selected from I for subsequent application.

In this study invariants are mined *offline*. Data available at t_0 consist of the entire datasets described in Section 3; no more data are fed to the framework beyond the datasets at t_0. It should be noted that invariant *mining* and *application* do not interfere with the system operations because they work on attributes extracted from the monitoring data.

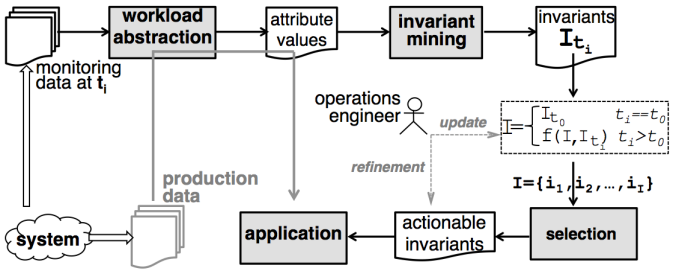

Fig. 3: Framework to mine invariants and feedback mechanisms.

4.1 Workload Abstraction

A well-known concern in training and validating models used by analysis techniques is the availability of the *ground truth* (also known as *class* or **label**) for a data point [25]. The knowledge of the label allows to *(i)* apply supervised techniques (decision list, in this study), for comparison with unsupervised ones, and *(ii)* carefully validate the findings.

We classify a workload unit to be **correct**, when it is correctly executed by the system, **anomalous** otherwise. The Google dataset indicates explicitly whether a job execution was correct, and contains information about how many times tasks were resubmitted. In the SaaS dataset, processing stages of transactions have an exit code and an explanation; the assignment of the ground truth (correct or anomalous) was done by the operation engineers.

4.1.1 Google dataset

The workload units consist of **jobs**, made of tasks. After filtering out a small number of inconsistencies (e.g. malformed records and blank attributes), we count 649,959 jobs. Of these, 372,688 are *finished*, 267,464 are *killed*, and 9,807 are *failed* jobs. We consider finished jobs as the *correct* class; killed and failed jobs build the *anomalous* class. We characterize jobs by means of attributes - a common practice in job-level analysis [26]. Attributes are:

- Tasks (T): number of tasks pertaining the job;
- Priority (P): priority of the job;
- Resubmissions (R): number of resubmissions of the tasks until the completion of the job;
- Duration (D): total duration of the job;
- CPU usage (C): average CPU usage of the job;
- Server (S): the type of server(s) the tasks run on.

The values of the attributes of a job are extracted from the tables described in Section 3.1. For practical mining purposes, the huge space of numerical values taken by the attributes is mapped to *categorical* values, beforehand. Categorization is usually done in empirical assessments for summarizing workload parameters through a small number of actionable classes (e.g., *low*, *moderate*, *medium*, *high*), which can be easily applied/understood by practitioners [27]. In order to establish the categories we analyze the distribution of the attributes, beforehand.

The frequency of tasks, resubmissions, CPU usage and duration follows a strong *power-law* distribution. This finding has been also noted for the same dataset by Di et al. [18] in their jobs characterization, and in the failure analysis in [19]. Fig. 4a-4c show the cumulative distribution function (CDF) of tasks, resubmissions and CPU usage. For example, Fig. 4a plots the probability p a job consists of no more than t tasks. It is worth noting that the majority of jobs contains a relatively small number of tasks (e.g., the probability a job has no more than 100 tasks is 0.9457). Similarly, Fig. 4b indicates that the probability a job experiences no resubmissions is 0.9187.

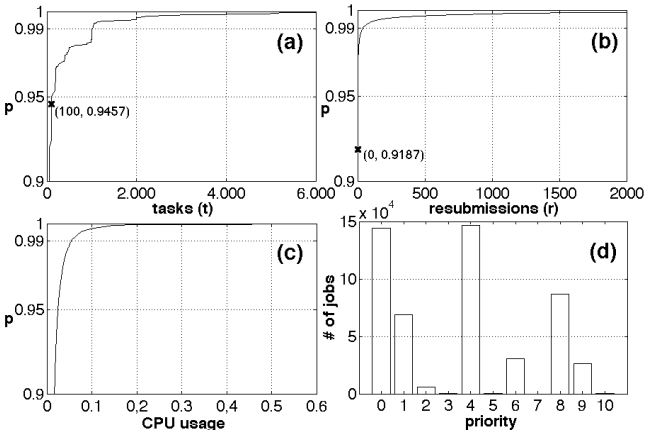

Fig. 4: Cumulative distribution function (CDF) of tasks, resubmissions and CPU usage; number (#) of jobs by priority value.

TABLE 2: Google dataset: Attributes and ranges of values.

Tasks (T) **(IG: 0.2071)**		Resub. (R) **(IG: 0.115)**		Priority (P) **(IG: 0.119)**	
V_T	*range*	V_R	*range*	V_P	*range*
T0	[0;10]	R0	0	low	[0;3]
T1	]10;1K]	R1	]0;100]	medium	[4;7]
T2	]1K;5K]	R2	]100;1K]	high	[8;11]
T3	]5K;+∞[	R3	]1K;+∞[		
Duration (D) **(IG: 0.113)**		CPU (C) **(IG: 0.007)**		Server (S) **(IG: 0.181)**	
V_D	*range*	V_C	*range*	V_S	
D0	[0;50]	C0	[0;0.05]	A	B
D1	]50;100]	C1	]0.05;0.1]	AB	BC
D2	]100;1K]	C2	]0.1;0.2]	ABC	C
D3	]1K;+∞[	C3	]0.2;+∞[	AC	

We use *four* categories ($X0$ to $X3$) to discretize T, D, R and C. Table 2 shows the mapping between the categorical and the original values of the attributes (P and S will be discussed later on in this Section). For instance, T assumes the categorical values $V_T = \{T0, T1, T2, T3\}$, whose ranges are shown in the second column: a job consisting of 8 tasks resubmitted 10 times until completion is assigned the values *T0* and *R1* for T and R, respectively. Attributes have been discretized in a way to preserve the inherent power-law variability of the data as follows. Fig. 4a-4c suggest that the CDFs (i) increase sharply when the value of the attribute is small and (ii) start flattering until they converge to 1 over a very wide range of values. For each attribute T, D, R and C, the category $X0$ catches the initial increase of the CDF, while $X3$ corresponds to the range of values where the CDF is almost flat; $X1$ and $X2$ cover the range of values before and after the *knee-point*, which characterizes the transition of the CDF from the sharp initial increase to the flat part.

Priorities (P) have been grouped in *low* (0-3), *medium* (4-7) and *high* (8-11). Fig. 4d shows the number of jobs by priority, which suggests our discretization suits well the data. The *type of server* (S) is categorical. There exists three types of servers - A, B and C: the tasks of a job are allocated to one or more of these servers. The servers are listed in the *Machine_attribute* table; Garraghan et al. [28] describe how the types can be mapped to physical machines. Values of V_S in Table 2 were inferred based on the server(s) the job was allocated to for execution.

It is worth investigating whether potential relationships among jobs influence the data precision. To this aim we measured the information content of the attributes through the notion of **information gain** [29], used here to quantify the *usefulness* of the attributes at predicting the label of the jobs (finished, killed, failed). The gain (IG) per attribute is in Table 2. We believe that no small subset of attributes predominates at predicting the label, and we decided to keep all attributes in the mining step.

Sensitivity analysis. The percentage of jobs falling into the categories of a given attribute (referred to as *percentage cardinality* in the following) depends on the ranges. For example, with the ranges in Table 2, *T0*, *T1*, *T2* and *T3* contain the 76.64, 22.38, 0.93 and 0.05% of the total jobs, respectively. Although we arranged the categories in a way to preserve the original power-law variability of the attributes, a different selection of the ranges might impact the cardinality and, in turn, invariants-related inferences made on the categories. We assess the **sensitivity** of the cardinality with respect to variations of the ranges shown in Table 2.

The assessment has been done as follows. It should be noted that the ranges are uniquely determined by three *bounds*, i.e., b_1, b_2, and b_3. For example, the bounds of T and C are 10, 1K, 5K and 0.05, 0.1, 0.2, respectively. Given an attribute and the bounds b_i (i=1,2,3), we compute the cardinality of the categories for each $b_i \pm \frac{b_i}{100} \cdot \Delta$ (with Δ=[5;50] by step 5). In other words, for each percentage variation Δ we collect 6 observations per category. Fig. 5 summarizes the results of the sensitivity analysis (y-axis is in *log-scale* to better visualize $X2$ and $X3$). The dotted lines represent the percentage cardinality of each category, obtained using the bounds in Table 2; any other data point is the percentage cardinality of a given category subject to the percentage variation of the bounds reported by the x-axis. For example, when the bounds of *tasks* vary by 50% (i.e., b_1=[5;15], b_2=[500;1,500] and b_3=[2,500;7,500]) the average cardinality of *T0*, *T1*, *T2* and *T3* is 77.66, 21.26, 1.01 and 0.07% (Fig. 5a), which is close to the above-mentioned values obtained through the ranges in Table 2. Similarly, the cardinality of *C2* and *C3* (Fig. 5c) - which would seem the most variable categories due to the log scale - is 0.25 and 0.012 with our ranges selection, and, on average, 0.34 and 0.052 under a 50% variation of the bounds. The results suggest that the variation of the bounds does not significantly impact the cardinality of the categories. In this respect, it can be reasonably stated that the results presented hereinafter for the Google dataset hold under different selections of the bounds.

4.1.2 SaaS dataset

The workload unit in the SaaS dataset is the **processing stage** of a transaction. We abstracted the processing stage through the following attributes, available in the *Details* audit log (Table 1):

- Stage (S): the name of the processing stage;
- Exit code (E): the outcome returned at the end completion of the stage (i.e., *Status* column);
- Reason (R): the reason leading to a given exit code (i.e., *Fail Reason* column).

Table 3 lists the top-8 occurring values of the stage (S) attribute, the four possible exit codes (E), and typical reasons (R) encountered in the dataset. Differently from the previous dataset, all the attributes are categorical in the SaaS log. The label of each

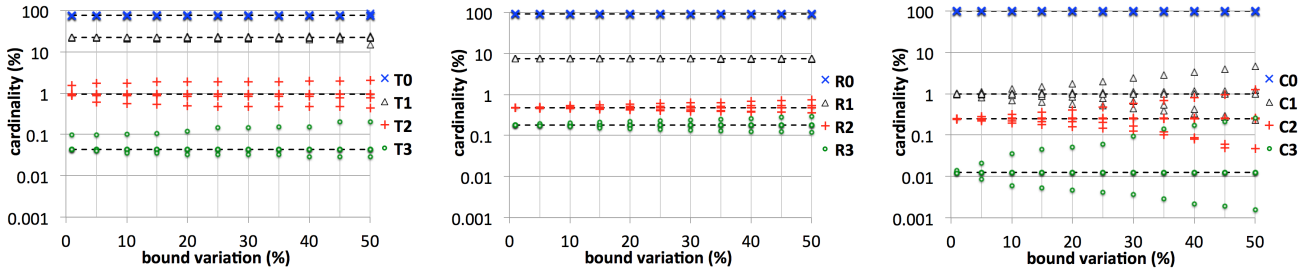

(a) Tasks. (b) Resubmissions. (c) CPU Usage.

Fig. 5: Sensitivity of the cardinality (%) with respect to the percentage variations of the bounds of the categories.

TABLE 3: SaaS dataset: Attributes and samples of values.

Stage (S): V_S		Exit (E): V_E	Reason (R): V_R
IT3	IT4_L1	L1_REJ	Invalid_File
IT3_PVLD	IT4_TRNF	L2_REJ	System_Error
IT4	IT4_STG	SE	Move_Failed
IT4_L2	IT5	MIN_PP	Corrupt_File

processing stage (either *correct* or *anomalous*), which denotes the correctness of its execution, has been provided by the experts of the IT company operating the SaaS platform. The execution is anomalous (i.e., the stage belongs to the *anomalous* class) if *(i)* reason is *NULL* when the stage exits with code *L1_REJ* or *L2_REJ*; *(ii)* the exit code is not *L1_REJ* when the processing stage is *IT4_L1* and reason is *File_Validation_Failure*. Out of total 30,025 processing stages executions, 3,299 were anomalous.

4.2 Mining Techniques

The **invariant mining** step shown in Fig. 3 aims to infer recurring patterns among the attributes of the workload units. Likely patterns represent invariants, i.e., properties holding across different executions of batch work.

Let us clarify the notion of invariants through examples. In the Google dataset we noted that 54,976 jobs assume the values *R0*, *low* and *D0* for attributes R, P, and D, respectively, meaning that a significant number of jobs experiencing no task resubmissions have low priority and small duration. Similarly, in the SaaS dataset, 10,701 processing stages assume the value *IT3*, *L1_REJ*, *Invalid_File* (for S, E and R, respectively), indicating that the stage IT3 exiting with code L1_REJ fail because of an *invalid file*.

There are a number of considerations underlying the choice of the **clustering**, **association rules** and **decision list** mining techniques. First, production systems might generate *unlabeled* workload data, which prevents the use of many machine learning techniques. More important, as pointed out in [1], invariants should be comprehensible and useful to practitioners. Alternative invariant-based classifiers can been applied, e.g. neural or Bayesian networks; however, their output, e.g., probabilities and/or weights, have small explicative power for practical purposes.

4.2.1 Clustering

The values of the attributes of each workload unit identify a point in a N-dimensional space. Fig. 6 shows the 3D scatterplot of all processing stages available in the SaaS dataset. It can be noted that the 30,025 stage concentrate around a few tens data points. A similar consideration can be done in the Google dataset. This technique identifies clusters (also known as groups) of data points. The technique has been applied through the well established algorithms **K-medoids**[2] [30] and Density Based Spatial Clustering of Applications with Noise (**DBSCAN**) [31].

The number of clusters K the workload units will be assigned to is an input parameter of K-medoids. The larger K, the finer the clustering. The *medoid* of a cluster (representing its center) is assumed to be the invariant that characterizes the data points of the cluster. DBSCAN overcomes a number of limitations in clustering large datasets: for instance, it does not require the knowledge of the input number of clusters, it can discover clusters with arbitrary shapes, and it encompasses the notion of noise.

2. K-medoids is a generalization of the K-means algorithm, which addresses both numerical and categorical data.

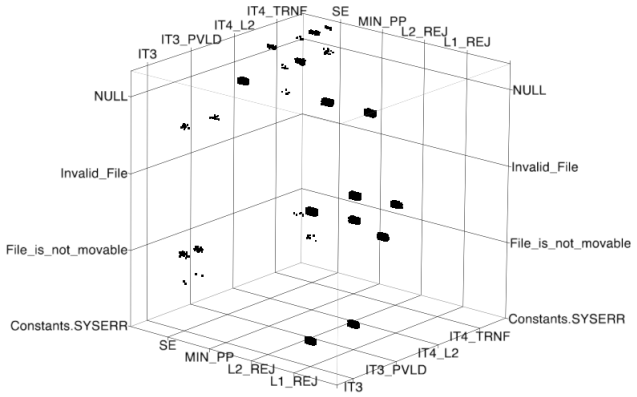

Fig. 6: 3D scatterplot of the workload units in the SaaS dataset.

We assume that the points belonging to the same cluster are characterized by the same invariant. Clusters are sorted by decreasing size, beforehand: likely invariants are deemed to be the ones representing larger clusters. Clustering is an *unsupervised* technique (i.e., it does not require labelled training data). The invariants obtained specify the values of all the attributes.

4.2.2 Association Rules

The second technique is *frequent itemset mining*, which extracts frequently observed patterns in a database in the form of *itemsets* or **association rules**. This technique is well known in the field of market basket analysis, where it is used to find out sets of products that are frequently bought together [32]. We apply the *association* concept to values of attributes.

Let $B = \{i_1, ..., i_m\}$ be a set of items, any $S \subseteq B$ an *itemset*, and T the *bag of transactions* under consideration (a *transaction* is a set of items). The *absolute support* (the *relative support*) of S is the number of transactions in T (the percentage of transactions in T) that contain S. More formally, let $U = \{X \in T \mid S \subseteq T\}$ be the set of transactions in T that have S as a subset (i.e., contain all the items in S and possibly some others). Then $suppabs(S) = |U| = |\{X \in T | S \subseteq T\}|$ is the absolute support of S, and $supprel(S) = \frac{|U|}{|T|} \times 100\%$ is the relative support of S. Here $|U|$ and $|T|$ are the number of elements in U and T, respectively.

In this study, **Apriori** [33] and Generalized Sequential Patterns (**GSP**) [34] are used to mine association rules. The attributes matrix constructed through the *workload abstraction* step in Fig. 3 is assumed to be the above-mentioned bag of transactions T (i.e., each row of the matrix is a transaction).

We use Borgelt's implementation of Apriori [35], which returns the *maximal itemsets* in T whose relative support is larger than a threshold. The **support threshold** (s) is an input of the algorithm: the smaller it is, the larger the number of association rules that will be returned by the algorithm. Differently from Apriori, GSP performs different scans over T. At any scan k (with k>1) GSP generates a set of *candidate* k-sequences from frequent (k-1)-sequences; candidate k-sequences undergo a pruning step. GSP stops when no more frequent sequences are found.

Association rules returned by either Apriori or GSP are assumed to represent an invariant. Rules are sorted by decreasing values of the support, i.e. by decreasing likelihood.

4.2.3 Decision List

A decision list is an ordered set of classification rules. Given a workload unit abstracted by the value of the attributes, the list is scanned until a rule is found that matches the attributes: the label

of the unit is assumed to be the one indicated by the rule. We use two different algorithms to obtain a decision list. The former is partial-decision-trees-based (**PART**) [36], combining the best of C4.5 and RIPPER, which represent the primary approaches to rule-based learning. The latter is the Decision Table / Naive Bayes (**DTNB**) [37] algorithm, which combines a naive Bayes approach with induction of decision tables.

Fig. 7 lists some of the 91 classification rules obtained for the Google dataset with PART. For instance, a job where T=*T2* and R=*R0* is classified as `KILLED` regardless the value of the remaining attributes because it matches the rule at *line 2*; similarly, by looking at *line 4* and *6* it can be noted that a job where T=*T0* and R=*R0* and P=*High* and D=*D2* is classified as `FINISHED` if *(i)* it has been run on the server type B (regardless the CPU usage) or *(ii)* its CPU usage has been *C0* in the case the server type is C.

Differently from clustering and association rules, decision list is a supervised technique because the model is learned from a labeled dataset (i.e., beside the attributes matrix, the construction of the tree requires the knowledge of the label of each workload unit). In this study, the rules in the list that aim to catch the *correct* workload units are deemed to be invariants; they are sorted by decreasing number of correct units they detect.

```
1  if (T=T2 and R=R1) then KILLED
2  else if (T=T2 and R=R0) then KILLED
3  //omitted
4  else if (T=T0 and R=R0 and P=High and D=D2 and S=B)
5          then FINISHED
6  else if (T=T0 and R=R0 and P=High and D=D2 and C=C0
7          and S=C) then FINISHED
8  //omitted
9  else if (P=MEDIUM) then FAILED
10 default FINISHED
```

Fig. 7: Examples of decision list rules for the Google dataset.

5 Evaluation Metrics

The set of invariants $I = \{i_1, i_2, \ldots, i_I\}$ returned by a mining technique is assessed through widely established information retrieval metrics, in order to quantify to what extent the invariants are able to *(i)* abstract recurring properties of the executions of workload units (i.e., *jobs* or *processing stages*), and *(ii)* discriminate correct/anomalous executions. The invariants in I are sorted by **likelihood**, beforehand (as discussed in Section 4.2). We assess how the metrics vary by using a progressively increasing number of *less-likely* invariants from I: this strategy allows to establish the number of invariants that properly characterize a dataset.

Let s_i ($1 \leq i \leq I$) denote the subset of the top-i invariants. For example, in the case $I = \{i_1, i_2, i_3, i_4\}$ four sets are obtained, i.e., $s_1 = \{i_1\}$, $s_2 = \{i_1, i_2\}$, $s_3 = \{i_1, i_2, i_3\}$, $s_4 = \{i_1, i_2, i_3, i_4\}$. It can be noted that s_i ranges between the sets $\{i_1\}$ and I, denoting the most likely invariant and all the invariants in I, respectively. Each subset s_i is run against the input dataset. A workload unit in the dataset is assigned to one out of four disjoint classes based on the result of the comparison between the *(i)* label and *(ii)* outcome of the invariant-based checking. The sets (Fig. 8) are:

- **true negative (TN)**: the workload units (W) with label *correct* and matching at least one invariant in s_i;
- **false negative (FN)**: set of W with label *anomalous* and matching at least one invariant in s_i;
- **false positive (FP)**: set of W with label *correct* and matching no invariant in s_i;
- **true positive (TP)**: set of W with label *anomalous* and matching no invariant in s_i.

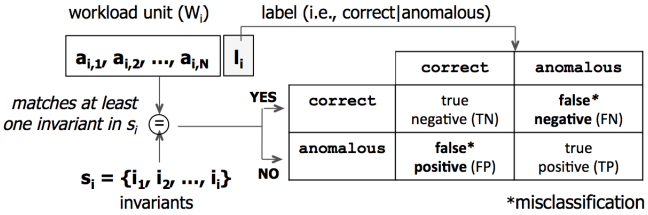

Fig. 8: Confusion matrix.

Given s_i, we compute the **coverage** (C) as the ratio between the number of workload units matching at least one invariant in s_i and the total number of workload units, and **specificity** (S), **recall** (R), and **precision** (P) as follows:

$$S = \frac{|TN|}{|correct|} \quad R = \frac{|TP|}{|TP| + |FN|} \quad P = \frac{|TP|}{|TP| + |FP|} \quad (1)$$

Specificity is the ratio between the number of correct workload units detected by s_i and the total number of correct workload units. *Recall* is the probability that an anomalous workload unit is detected by s_i. *Precision* is the probability that a workload unit, which matches no invariant in s_i, is actually anomalous. *Coverage* can be computed also for unlabeled datasets.

Let us present an example. The use of *clustering* with K=10 for the Google dataset returns the invariants listed in Table 4 by decreasing likelihood.

TABLE 4: Google dataset: invariants mined by *clustering* (K=10).

i_1	*Low, D2, T0, C0, c, R0*	i_6	*High, D0, T0, C0, c, R0*
i_2	*Med, D2, T1, C0, bc, R0*	i_7	*Med, D0, T0, C0, c, R0*
i_3	*Med, D2, T0, C0, c, R0*	i_8	*High, D1, T0, C0, c, R0*
i_4	*Low, D0, T0, C0, c, R0*	i_9	*Med, D3, T1, C0, abc, R0*
i_5	*High, D3, T0, C0, c, R0*	i_{10}	*Med, D2, T1, C0, abc, R0*

Based on these, it is possible to build 10 subsets s_i, whose C, S, R, P are listed in the four rightmost columns of Table 5. Since invariants in I are ordered by decreasing likelihood, the cardinality of s indicates the invariants of I being assessed. For instance, s_3 consists of the three most likely invariants {(*Low, D2, T0, C0, c, R0*), (*Med, D2, T1, C0, bc, R0*), (*Med, D2, T0, C0, c, R0*)}, namely i_1, i_2 and i_3 in Table 4. They match a total of 160,560 jobs (|TN| + |FN|), with a coverage of 0.25; the specificity *S* equals 0.15 because s_3 detects 57,117 TNs out of total 372,688 negatives. The use of two further invariants, i.e. s_5, would increase the coverage from 0.25 to 0.38.

Throughout the rest of the paper we use the type of plots in Fig. 9 to summarize the metrics for a set of invariants I. Fig. 9a shows how coverage/specificity vary with the number of invariants in I: the plot is useful to appreciate the number i of the top-i invariants in I, which contribute most to the characterization

TABLE 5: Google dataset: values of the evaluation metrics for invariants of Table 4.

s	|TN|	|FP|	|FN|	|TP|	C	S	R	P
1	38834	333854	64616	212655	0.16	0.10	0.77	0.39
2	40118	332570	94712	182559	0.21	0.11	0.69	0.35
3	57117	315571	103443	173828	0.25	0.15	0.63	0.36
4	108947	263741	105323	171948	0.33	0.29	0.62	0.39
5	135143	237545	111570	165701	0.38	0.36	0.60	0.41
6	162504	210184	114560	162711	0.43	0.44	0.59	0.44
7	194599	178089	114697	162574	0.48	0.52	0.59	0.48
8	218457	154231	117294	159977	0.52	0.58	0.58	0.51
9	218587	154101	118705	158566	0.52	0.59	0.57	0.51
10	218763	153925	124958	152313	0.53	0.59	0.55	0.50

This article has been accepted for publication in a future issue of this journal, but has not been fully edited. Content may change prior to final publication. Citation information: DOI 10.1109/TSC.2017.2679715, IEEE Transactions on Services Computing

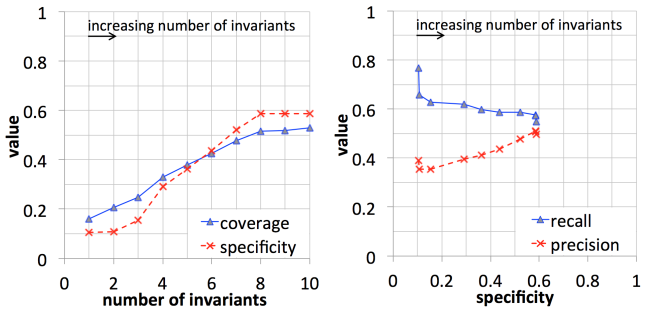

(a) Coverage/specificity wrt the number of invariants.

(b) Recall/precision wrt the specificity.

Fig. 9: Plots to analyze the results of Table 5.

of executions. Fig. 9b shows how precision/recall vary with the specificity: the plot allows appreciating the tradeoff between the number of correct executions detected by I and the goodness of the detection. Fig. 9 summarizes the values in Table 5: for example, for the subset s_3 discussed above, in Fig. 9a we see C=0.25 and S=0.15; for s=0.15 (x-axis) in Fig. 9b, we obtain R and P of the three invariants in s_3 (0.63 and 0.36, respectively).

6 Applications

The techniques are investigated in the context of two typical applications of invariant-based analysis, namely **executions characterization** and **anomaly detection**. We establish the best set of invariants returned by K-medoids and Apriori through a sensitivity analysis, beforehand; the comparison with the remaining algorithms is presented in Section 6.2 and 6.3.

6.1 Sensitivity Analysis

We assess the **sensitivity** of K-medoids and Apriori with respect to the input parameters K (number of clusters) and s (relative support threshold), respectively. For example, in the Google dataset the Apriori algorithm set with s=38% returns the invariants $\{(T0,C0,c,R0), (D2,C0,R0), (Low,C0), (D2,T0,C0)\}$; invariants change to $\{(T0,C0,c,R0), (Low,T0,C0), (Low,C0,R0), (D2,T0,C0,R0), (D2,C0,c,R0), (Low,C0,c)\}$ if s=35%. Lowering the support by 3% results into different sets of invariants.

For the **Google dataset**, Fig. 10a and 10e show how recall and precision vary with respect to the specificity for invariants obtained under different values of K. Analysis has been done with $2 \leq K \leq 20$ by step 2; however, Fig. 10a and 10e show the results for K=8,12,14,18 for better visualization. For example, the top-3 invariants obtained by means of K-medoids with K=12 (i.e., full blue, △-marked, series - third point from the left) have S=0.25, R=0.65, P=0.39; on the other hand, the top-3 invariants in K=8 (i.e., dotted grey, □-marked, series - third point from the left) have S=0.22, R=0.71, P=0.40. An optimal set of invariants, - the one resulting into the best recall/precision with respect to specificity - is obtained with K=14 (i.e., dotted black, ×-marked, series).

For any value of K, Fig. 10a indicates that recall (R) is a monotonic decreasing function of the specificity. As shown by Eq. 1, while the denominator of R is constant regardless the number of invariants (|TP|+|FN| is the total number of anomalous workload units), the numerator of R, i.e., |TP|, decreases as specificity increases[3]. Differently from recall, precision (P) might either increase or decrease with the specificity.

Fig. 10b and 10f show recall and precision of the invariants obtained through Apriori with different values of the support threshold. Again, we explore values of the support generating from 2 to 20 invariants by step 2; however, a smaller subset is shown for the sake of clarity. As a result, we choose the invariants obtained with s=6% (dotted black, ×-marked, series).

For the **SaaS dataset**, Fig. 10c and 10g show recall and precision of the invariants mined by K-medoids with K=8,10,12. The best set is obtained with K=10 (dotted black, ×-marked, series). On the other hand, s=12% is the value of the support that allows obtaining the best set of invariants through Apriori, as it can be noted from Fig. 10d and 10h (dotted grey, □-marked, series).

3. The larger the number of invariants (and the coverage), the smaller the number of workload units that will be classified as anomalous (i.e., positive).

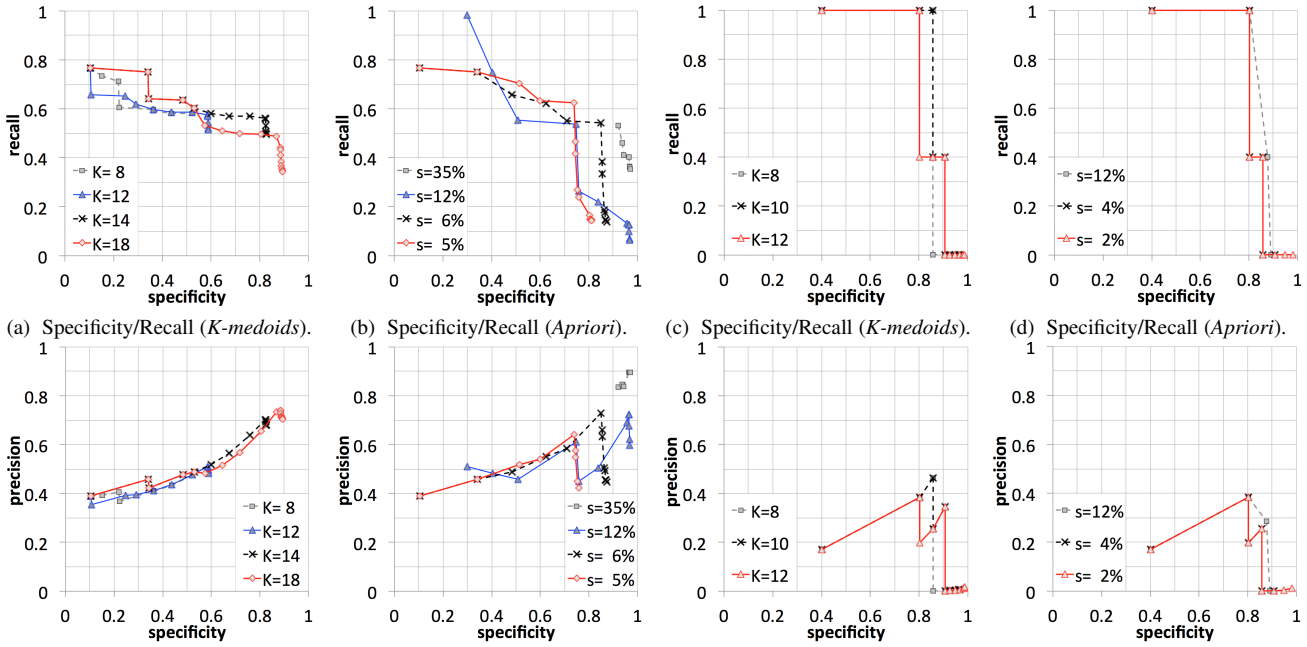

(a) Specificity/Recall (*K-medoids*).

(b) Specificity/Recall (*Apriori*).

(c) Specificity/Recall (*K-medoids*).

(d) Specificity/Recall (*Apriori*).

(e) Specificity/Precis. (*K-medoids*).

(f) Specificity/Precis. (*Apriori*).

(g) Specificity/Precis. (*K-medoids*).

(h) Specificity/Precis. (*Apriori*).

Fig. 10: Sensitivity of *K-medoids* and *Apriori* with respect to K and s. Google dataset: (a), (b), (e), (f); SaaS dataset: (c), (d), (g), (h).

6.2 Executions Characterization

We assess to what extent the invariants returned by the techniques hold across the executions of different workload units. To this aim, coverage and specificity are measured. Table 6 and 7 report the 6 (for Google) and 3 (for SaaS) most likely invariants returned by the algorithms, respectively. The invariants mined by K-medoids, DBSCAN and DTNB indicate the value of all the attributes; Apriori, GSP and PART might specify only some attributes.

TABLE 6: Google dataset: top-6 invariants mined by algorithms.

K-medoids (K=14)			
i_1	*Low, D2, T0, C0, c, R0*	i_4	*Low, D0, T0, C0, c, R0*
i_2	*High, D2, T0, C0, c, R0*	i_5	*Med, D2, T0, C0, c, R0*
i_3	*Med, D2, T1, C0, bc, R0*	i_6	*High, D3, T0, C0, c, R0*
DBSCAN			
i_1	*Low, D2, T0, C0, c, R0*	i_4	*Low, D1, T0, C0, c, R0*
i_2	*High, D2, T0, C0, c, R0*	i_5	*High, D3, T0, C0, c, R0*
i_3	*Low, D0, T0, C0, c, R0*	i_6	*Med, D0, T0, C0, c, R0*
Apriori (s=6%)			
i_1	*Low, D2, T0, C0, c, R0*	i_4	*Med, T0, C0, c, R0*
i_2	*High, D2, T0, C0, c, R0*	i_5	*D3, T0, C0, c, R0*
i_3	*D1, T0, C0, c, R0*	i_6	*Low, D0, T0, C0, c, R0*
GSP			
i_1	*D2, T0, C0, c, R0*	i_4	*T0, C0, c, R0*
i_2	*D0, T0, C0, c, R0*	i_5	*D2, T0, C0, R0*
i_3	*D2, T1, C0, bc, R0*	i_6	*D2, C0, c, R0*
PART			
i_1	*High, D2, T0, C0, c, R0*	i_4	*High, D0, T0, C0, c, R0*
i_2	*Low, D0, R0*	i_5	*High, D3, T0, C0, c, R0*
i_3	*Med, D0, T0, c, R0*	i_6	*High, T0, C0, c, R0*
DTNB			
i_1	*High, D2, T0, C0, c, R0*	i_4	*Med, D0, T0, C0, c, R0*
i_2	*Low, D0, T0, C0, c, R0*	i_5	*High, D0, T0, C0, c, R0*
i_3	*High, D3, T0, C0, c, R0*	i_6	*High, D1, T0, C0, c, R0*

TABLE 7: SaaS dataset: top-3 invariants mined by algorithms (IF: Invalid_File; FVF: File_Validation_Failure).

	K-medoids (K=10)		**DBSCAN**
i_1	*IT3, IF, L1_REJ*	i_1	*IT3_PVLD, IF, L1_REJ*
i_2	*IT3_PVLD, IF, L1_REJ*	i_2	*IT3, IF, L1_REJ*
i_3	*IT4_L2, FVF, L2_REJ*	i_3	*IT4, NULL, L2_REJ*
	Apriori (s=12%)		**GSP**
i_1	*IT3_PVLD, IF, L1_REJ*	i_1	*IF, L1_REJ*
i_2	*IT3, IF, L1_REJ*	i_2	*FVF, L2_REJ*
i_3	*L2_REJ*	i_3	*NULL, L2_REJ*
	PART		**DTNB**
i_1	*IF*	i_1	*IT3_PVLD, L1_REJ*
i_2	*FVF, L2_REJ*	i_2	*IT3, L1_REJ*
i_3	*FVF, L1_REJ*	i_3	*IT4_L2, L2_REJ*

Fig. 11 shows how the **coverage** varies with respect the number of invariants by technique and dataset. For each n along the x-axis, the y-axis is the value of the coverage achieved by the n most likely invariants. For example, the most likely 5 invariants returned by Apriori obtain a coverage of 0.60 in Google as it can be noted from Fig. 11b (△-marked series), i.e., they hold in 389,029 out of total 649,959 job executions; similarly, the most likely 3 invariants returned by K-medoids in SaaS hold in 22,912 out of 30,025 processing stages, i.e., coverage is 0.76, such as shown by Fig. 11d (△-marked series).

The plots indicate that, for any technique/dataset, coverage flattens sharply after a relatively small number of invariants (i.e., roughly 8-9 in Google and 2-3 in SaaS): the use of an arbitrary large number of invariants does not help improving coverage significantly. For example, K-medoids starts flattening at the 9*th*

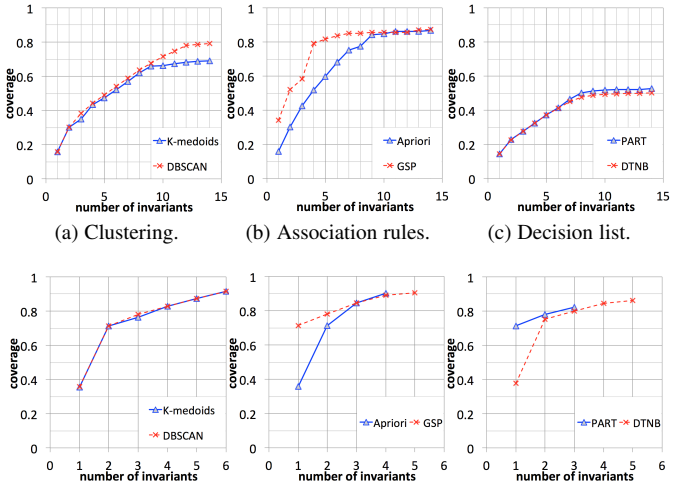

(a) Clustering. (b) Association rules. (c) Decision list.

(d) Clustering. (e) Association rules. (f) Decision list.

Fig. 11: Coverage of the techniques: Google (a-c), SaaS (d-f).

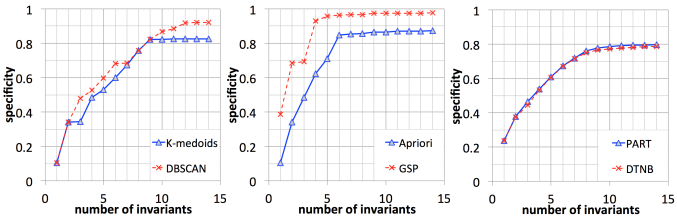

(a) Clustering. (b) Association rules. (c) Decision list.

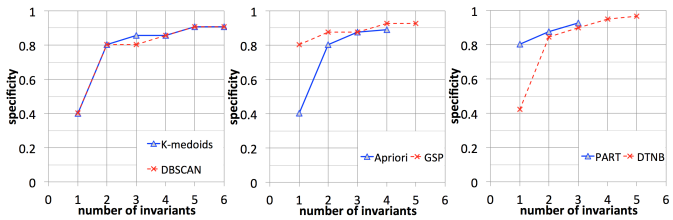

(d) Clustering. (e) Association rules. (f) Decision list.

Fig. 12: Specificity of the techniques: Google (a-c), SaaS (d-f).

invariant in Google, where coverage is 0.66: 5 more invariants contribute to increase the coverage by only 0.03, i.e., data point (14, 0.69) - K-medoids in Fig. 11a; similarly, the coverage of the top 4 GSP invariants in Google is 0.79, while 10 more invariants contribute to increase the coverage by roughly 0.1, i.e., Fig. 11b. The techniques achieve a rather different maximum coverage in Google, which ranges from 0.50 (DTNB) to 0.87 (Apriori).

In spite of the different coverage, the techniques converge to similar **specificity** (coverage of the *correct* executions), roughly 0.85 for Google and 0.9 for SaaS (Fig. 12). For instance, the coverage of PART is about 0.53 for Google, and its specificity is 0.8, i.e. 80% of correct executions match some invariant. The maximum specificity (0.97) is observed with GSP. No *few-fits-all* invariants can reasonably be mined for all the correct executions.

6.3 Anomaly Detection

Likely invariants have been used in past studies for anomaly detection. Properties that are likely invariants hold in regular operating conditions; their violation is considered symptom of execution malfunctions. This is a common practice in *unsupervised* learning, where the assumption is made that correct instances are far more likely than anomalies [25].

This article has been accepted for publication in a future issue of this journal, but has not been fully edited. Content may change prior to final publication. Citation information: DOI 10.1109/TSC.2017.2679715, IEEE Transactions on Services Computing

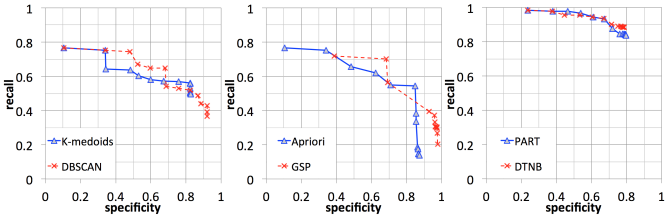

(a) Clustering. (b) Association rules. (c) Decision list.

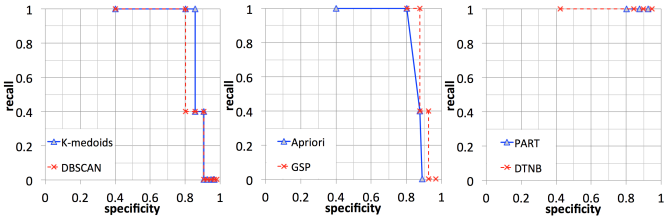

(d) Clustering. (e) Association rules. (f) Decision list.

Fig. 13: Recall of the techniques: Google (a-c) and SaaS (d-f).

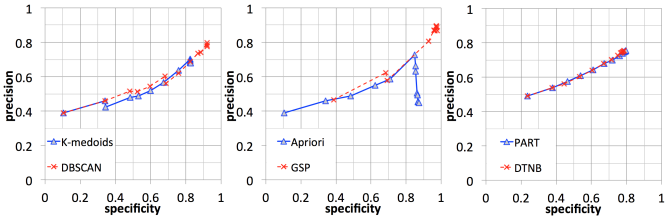

(a) Clustering. (b) Association rules. (c) Decision list.

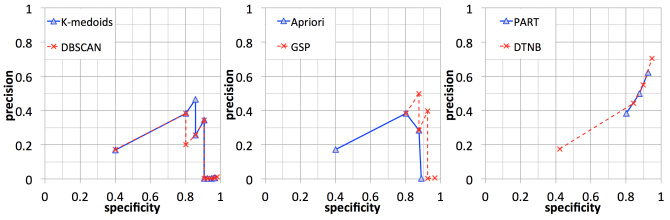

(d) Clustering. (e) Association rules. (f) Decision list.

Fig. 14: Precision of the techniques: Google (a-c) and SaaS (d-f).

The top invariants used for anomaly detection are shown in Tables 6 and 7. Fig. 13 plots how **recall** varies with respect to the specificity by technique and dataset. The plots indicate that, for any technique/dataset assessed in this study, recall decreases as the specificity (or, indirectly, the number of invariants) increases. Increasing the number of invariants allows inferring properties holding in more and more executions; however, it also increases the chance of *misclassifications* because it is likely that anomalous workload units will eventually match at least one invariant.

We plot recall (and, later, precision) with respect to the specificity rather than the number of invariants. This is because for the same number of invariants the techniques exhibit different coverage - as shown by Fig. 11. Rather than comparing them under different numbers of matching workload units, plotting recall/precision vs specificity allows to compare techniques when they match the same number of correct executions[4].

We observe that recall changes/converges *sharply* when the specificity is about 0.8-0.9. For example, the recall of the invariants returned by Apriori in the Google dataset drops from 0.54 to 0.15 when the specificity increases from 0.85 to 0.87, as it can be seen in Fig. 13b. This consideration applies also to clustering, where recall stops varying sharply. Recall decreases much more smoothly in *decision list*, until it stops at 0.8. These findings are confirmed in the SaaS datasets, i.e., Fig. 13d-13f. This suggests the possible existence of a *threshold phenomenon* in mining system invariants. Recall is strongly bound to the coverage of the correct executions; attempting to increase the specificity beyond a certain threshold (0.8-0.9 in our study), can strongly distort the recall.

Differently from the recall, **precision** of all the techniques increases as specificity increases; however, it stops, or even drops, sharply after having reached a maximum value. This can be clearly noted both in Fig. 14. Again, the threshold is represented by the value 0.8-0.9 of the specificity. Surprisingly, precision of supervised techniques, such as PART and DTNB, does not outperform unsupervised algorithms, such as the ones used for clustering or association rules mining. For example, in Google the maximum value of precision obtained by PART/DTNB is around 0.75, while precision of Apriori and K-medoids is 0.72 and 0.70. Although GSP might seem to achieve up to 0.89 precision, it must be noted that the recall corresponding to such precision is only 0.3; in practice the precision of GSP cannot by pushed beyond 0.62 without compromising the recall.

The workload units have been closely investigated to gain insights into recall and precision. We count the number of workload units that assume a given combination of values of attributes, i.e., *pattern*, in the following. Due to the larger variability of the data, we present the results from Google, for which we found out 565 distinct patterns. Fig. 15 shows the 100 most frequent patterns by decreasing number of workload units. A point along the x-axis denotes a pattern; the y-axis is the number of workload units assuming the pattern broken down by *correct* (i.e., *finished*), and *anomalous* (i.e., *killed* or *failed*) classes, in logarithmic scale. For example, total 53,710 workload units assume the values *(Low, D0, T0, C0, c, R0)*, being represented by *pattern #3* (third column from the left). The top-10 patterns (i.e., the first ten columns at the left side of the dotted vertical line in Fig. 15) sum up to 465,665 jobs. Although the most frequent patterns consist of almost all correct workload units (i.e., *finished* in Fig. 15), they might still contain a certain number of anomalous executions: invariants supposed to catch the frequent patterns will inadvertently misclassify anomalous executions, which affects the value of the recall. More important, a very long tail of patterns encompasses a significant number of correct executions. The remaining 555 patterns in Fig. 15 (i.e., right side of the dotted vertical line) account for total 47,053 correct executions. In order to correctly classify these executions, invariants should be able to depict such a large number of patterns. However, unfrequent patterns, although correct, would not result into likely invariants: as a result, precision is impacted.

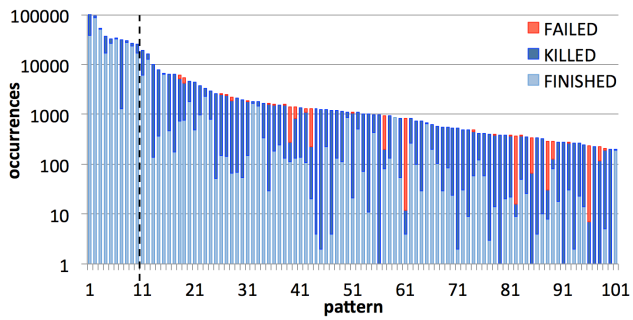

Fig. 15: Google dataset: number of workload units by pattern (occurrences are given in logarithmic scale).

4. Fig. 13 is very close to the *receiver operating characteristic* (ROC) curve; however, the x-axis is $specificity$ rather than $(1 - specificity)$ in order to visualize the effect of increasing number of invariants from left to right.

This article has been accepted for publication in a future issue of this journal, but has not been fully edited. Content may change prior to final publication. Citation information: DOI 10.1109/TSC.2017.2679715, IEEE Transactions on Services Computing

7 Practical Implications

Experimental results reveal pros and cons of widely-established techniques in invariant-based analysis. We leverage the results to infer practical implications that allow dealing with the concrete selection of likely invariants by operations engineers. We address the problems of *(i)* setting the input parameters of the mining algorithms (K-medoids and Apriori) *before* the analysis and *(ii)* selecting the optimal number of invariants out of the output produced by a mining algorithm. We propose a **heuristic** that can be used to select likely invariants. It is worth noting that our heuristic *does not* require labeled data: in this respect, it can be generally applied also to unlabeled datasets, where practitioners are expected to make decisions without the knowledge of metrics, such as recall and precision.

7.1 Invariants Selection

Invariants are inferred in two steps, i.e., *(i)* construction of I, i.e., the set of recurring properties (ordered by decreasing likelihood) among the attributes in a given dataset, and *(ii)* selection of a subset of invariants in I.

7.1.1 Setting of the mining algorithm

Algorithms, such as K-medoids and Apriori in this study, might require the setting of an input parameter to mine invariants. We measure how the invariants returned by an algorithm vary with respect to variations of the input parameter; measurements are used to infer an empirical rule that practitioners can use to set the input parameter *before* invariant-based analysis.

Difference between set of invariants is computed by means of the **Jaccard coefficient** (J_c). J_c is a widely adopted metric of *dissimilarity* between sets [38]; the use of J_c is well-known in clusters validation and quantifying feature similarities. The coefficient is used here as follows. Let I_1 and I_2 represent two sets of invariants. J_c is given by $(1 - \frac{|I_1 \cap I_2|}{|I_1 \cup I_2|})$, where $I_1 \cap I_2$ is the set of attribute values contained by both invariant sets I_1 and I_2, while $I_1 \cup I_2$ is the set of values contained by either I_1 or I_2. It should be noted that $I_1 \cap I_2$ and $I_1 \cup I_2$ contain no duplicated values by *notion* of set. J_c quantifies the dissimilarity of the invariants by means of the presence of given attribute values in I_1 and/or I_2. For example, let I_1 and I_2 be composed by the following 2 and 4 invariants, respectively: I_1={*(T0, C0, c, R0), (D2, C0, R0)*} and I_2={*(T0, C0, c, R0), (D2, C0, R0), (Low, C0), (D2, T0, C0)*}. The value of J_c is 0.167 (i.e., 1-5/6) because $I_1 \cap I_2$={*C0, D2, R0, T0, c*} and $I_1 \cup I_2$={*C0, D2, Low, R0, T0, c*}. If $I_1 == I_2$ the intersection of the sets is equal to their union: J_c=0. Conversely, if $I_1 \cap I_2 = \emptyset$, then J_c=1. Note that $0 \leq J_c \leq 1$; moreover, the larger J_c, the more diverse the sets of invariants.

Fig. 16 shows how J_c varies with respect to variations of the input parameter of the mining algorithms. Given a set I consisting of i invariants (i.e., i on the x-axis), the y-axis reports J_c measured between I and the output set produced by the algorithm, when it is configured in a way to return $(i - 2)$ invariants. The value of i=2 is set to 1 by construction; we tested the range 2-20 by step 2. For example, Fig. 16a indicates that when the number of invariants obtained through Apriori varies from 2 to 4, J_c goes from 1 to 0.167 (please note that this datapoint corresponds to the J_c example presented above); in order to discover two more invariants, i.e., 4 to 6, support must be decreased from 38.0% to 35.5% and J_c goes from 0.17 to 0, accordingly.

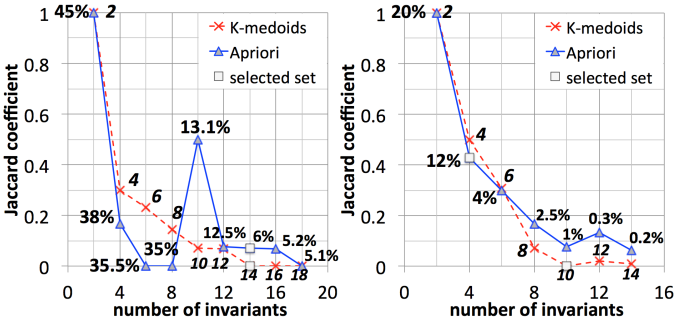

(a) Google. (b) SaaS.

Fig. 16: Value of J_c by technique/dataset (percentages denote supports; number of clusters, otherwise).

It can be noted that J_c decreases as the number of invariants increases, which indicates that the sets I start stabilizing (i.e., the values of the attributes that characterize the invariants become similar - small J_c -). In 3 out of 4 cases, the best set of invariants selected according to the sensitivity analysis presented in Section 6.1, i.e., grey, □-marked points in Fig. 16, correspond to small values of J_c, if not even 0, such as the case of K-medoids. As a *rule of thumb*, we suggest to run a mining algorithm under different values of the input parameters; values should be selected in a way to allow the algorithm to return a progressively increasing number of invariants. The computation of J_c between consecutive sets I highlights the value of the input parameter where invariants stabilize: according to our data, a good set of invariants is returned by a configuration of the input causing J_c to be small.

7.1.2 Number of invariants

Beside the *setting* problem, which occurs for those algorithms relying on an input parameter, practitioners are required to select a subset of likely invariants out of the output of *any* mining algorithm. Selecting the proper subset of invariants is **critical**: Fig. 11 and 12 indicate that few likely invariants contribute to increase coverage/specificity sharply; Fig. 13 and 14 suggest that recall and precision are negatively impacted by increasing values of the specificity. The problem of selecting invariants is even exacerbated in unlabeled dataset, where specificity/recall/precision cannot be computed. We address the problem as follows.

Experimental results provide reasonable evidence of the following **relationship** among number of invariants, coverage and classification-related metrics: *selecting a number of invariants where coverage is saturated, results in a value of specificity that corresponds to the threshold where recall and precision start decreasing sharply*. This can be noted across different techniques and datasets. We discuss a data point for the sake of clarity: the coverage of *K-medoids* in Google enters saturation at the 9*th* invariant, i.e., Fig. 11a. A number of invariants bigger than 9, e.g., 12, obtains a specificity of 0.83, i.e, Fig. 12a: the value 0.83 denotes the point of the x-axis in Fig. 13a and 14a where recall and precision of K-medoids have decreased/stopped sharply.

Let us denote **knee-point** of the coverage the number of invariants where coverage stops increasing significantly: the knee-point represents the beginning of the coverage *saturation*. For each dataset/technique, Table 8 shows the knee-points (*bold* character) and the points immediately before/after the knee, as it can be inferred from Fig. 11; moreover, the table shows the value of the metrics. It can be noted that, differently from a number of invariants taken where coverage is saturated, the knee-points represent a reasonably good tradeoff between recall and precision.

Accordingly, we propose the following **heuristic**: *a good number of invariants is indicated by the knee-point of the coverage*. The heuristic is generally applicable in practice because the computation of the coverage does not require the knowledge of the label.

We note that *association rules* are not the best suited for anomaly detection. Table 8 indicates that Apriori and GSP achieve the minimum recall for the datasets. Nevertheless, given the high coverage, *association rules* are still useful to characterize the system execution (e.g., to support workload characterization, usage profiling and capacity planning). On the other hand, *decision list* is strongly recommended for anomaly detection; however, it needs the label in order to be applied. *Clustering* might be used in place of decision list to deal with unlabeled datasets.

TABLE 8: Number of invariants selected through the *knee-point heuristic*, and values of evaluation metrics.

Google dataset					SaaS dataset				
n	C	S	R	P	n	C	S	R	P
K-medoids									
8	0.62	0.76	0.57	0.64	1	0.35	0.40	1	0.17
9	**0.66**	**0.82**	**0.56**	**0.70**	**2**	**0.71**	**0.80**	**1**	**0.38**
10	0.66	0.82	0.56	0.70	3	0.76	0.86	1	0.46
DBSCAN									
11	0.75	0.86	0.44	0.74	1	0.36	0.40	1	0.17
12	**0.77**	**0.92**	**0.43**	**0.79**	**2**	**0.71**	**0.80**	**1**	**0.38**
13	0.79	0.92	0.39	0.78	3	0.78	0.80	0.40	0.20
Apriori									
6	0.68	0.84	0.54	0.73	1	0.36	0.40	1	0.17
7	**0.75**	**0.85**	**0.38**	**0.66**	**2**	**0.71**	**0.80**	**1**	**0.38**
8	0.77	0.85	0.33	0.63	3	0.85	0.88	0.40	0.29
GSP									
3	0.58	0.69	0.56	0.58	-	-	-	-	-
4	**0.79**	**0.93**	**0.39**	**0.81**	**1**	**0.71**	**0.80**	**1**	**0.38**
5	0.82	0.96	0.37	0.87	2	0.78	0.88	1	0.50
PART									
7	0.47	0.72	0.87	0.70	-	-	-	-	-
8	**0.50**	**0.76**	**0.85**	**0.72**	**1**	**0.71**	**0.80**	**1**	**0.38**
9	0.51	0.78	0.85	0.74	2	0.78	0.88	1	0.50
DTNB									
7	0.45	0.72	0.90	0.70	1	0.38	0.42	1	0.18
8	**0.48**	**0.75**	**0.89**	**0.73**	**2**	**0.75**	**0.84**	**1**	**0.44**
9	0.49	0.77	0.89	0.74	3	0.80	0.90	1	0.55

7.2 Results Validation

The invariants selected with the proposed heuristic are used in the **Google dataset**. Fig. 17 shows the frequency distribution of the attribute values of the anomalous class (*killed* and *failed* jobs), comparing the *actual* distribution (i.e., actually anomalous jobs) to those obtained through K-medoids, GSP and DTNB. For example, the CPU usage of 271,283 actual anomalous jobs is C0; this value is 214,655 in K-medoids, 129,155 in GSP and 333,404 in DTNB. We note that DTNB infers a very similar distribution when compared to the *actual* data series: in fact anomaly detection done by means of this technique results into the maximum recall and precision (0.89 and 0.73, respectively), as shown in Table 8. These figures are consistent with [20], which proposes a failure prediction study of the Google dataset. At the other end of the spectrum, GSP produces a rather different distribution. For example, although *Low* is the most frequent priority value of anomalous jobs, GSP would erroneously suggest that the frequency of the priority values of anomalous jobs is similar. K-medoids allows preserving many of the characteristics of anomalous jobs. For example, differently form GSP, it correctly infers that *Low* is the most likely priority of anomalous jobs.

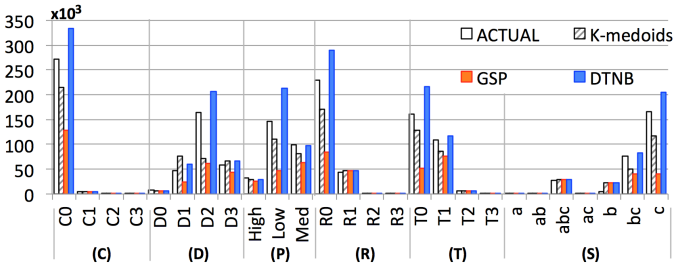

Fig. 17: Google dataset: frequency distribution of the attribute values of the *anomalous* workload units.

Similarly, we analyze the anomalies detected through invariants in the **SaaS dataset**. Discussion focuses here on *decision list*; however, similar results have been noted in the other techniques. The three invariants in Table 7 - i_1, i_2, i_3 (PART) - detect 5,293 anomalous processing stages executions. We group the stages assuming the same attribute values into the same class and obtain total 24 classes. Table 9 shows the classes, whose cardinality is reported by the leftmost column of the table. According to the notion of invariant, none of the classes in Table 9 matches i_1, i_2, i_3. For instance, in no case *Reason* in Table 9 is *Invalid_File*.

Each class has been carefully reviewed by the SaaS service operation experts of the IT company with the aim of validating the results. For example, the top two classes, which account for 1,981 and 1,321 instances, respectively, are true anomalies because they match the domain rules in Section 4.1.2. False anomalies are denoted by $\times$ in Table 9: as also noted in Google, correct executions that generate infrequent combinations of attributes will likely cause false positives. For example, this is the case of the classes assuming the value *File_already_exist* as *Reason*.

The experts team acknowledged that 5 out of 24 classes needed further investigation: they are denoted by '!' in Table 9. Beside the ones encompassed by the domain rules, invariant-based analysis detected total 461 stage executions reporting a *NULL* value for the *Reason*. Our analysis revealed that the stages exiting with the *SE* code might occasionally report no reason. Although this behavior of the SaaS platform was unnoticed until our study, the experts confirmed that it did not impact operations. On the contrary, 6 out of the above-mentioned 461 cases, i.e., the IT4, NULL, MIN_PP class in Table 9, were taken on high priority because they represented a silent data corruption leading to a system failure. The operations team confirmed that during the month of September 6 transactions were erroneously handled because of the missing *Reason* field from the processing stage. Overall, these findings were valuable to the service operation team.

8 Threats to Validity

As for any data-driven study, there may be concerns regarding the validity and generalizability of the results. We discuss them, based on the four aspects of validity listed in [39].

Construct validity. The study is based on two *independent*, real-world datasets, representative of two important categories of service computing platforms. Both sets contain data collected in operation under the natural workload/faultload, and encompass a total of about 680,000 data points concerning jobs, tasks and processing stages. The study builds on experiments aiming to infer possibly general insights, useful towards putting invariant-based techniques into common practice. This is pursued by considering well-established algorithms available in widespread

TABLE 9: Anomalies detected by *decision list* (PART) in SaaS with three likely invariants. Answer by the SaaS experts: true anomaly ($\surd$), false anomaly ($\times$), needed further investigation (!).

#	Stage	Reason	Exit code	Answer
1,981	IT4	NULL	L2_REJ	$\surd$
1,312	IT4	NULL	L1_REJ	$\surd$
555	IT3_PVLD	Corrupt_File	L1_REJ	$\times$
554	IT3	Corrupt_File	L1_REJ	$\times$
350	IT4	NULL	SE	!
154	IT4_TRNF	System_Error	SE	$\times$
92	IT4_L2	System_Error	SE	$\times$
79	IT4_STG	NULL	SE	!
35	IT5	Load_failed	SE	$\times$
28	IT3_P	File_is_not_movable	SE	$\times$
28	IT3	File_is_not_movable	SE	$\times$
24	IT5	System_Error	SE	$\times$
20	IT5	NULL	SE	!
19	IT4_STG	System_Error	SE	$\times$
12	IT3_PP	Move_Failed	SE	$\times$
12	IT3	Move_Failed	SE	$\times$
7	IT3_PVLD	Infected_File	L1_REJ	$\times$
7	IT3	Infected_File	L1_REJ	$\times$
6	IT4_PREP	NULL	SE	!
6	IT4_L1	File_Validation_Failure	MIN_PP	$\surd$
6	IT4	NULL	MIN_PP	!
2	IT6	System_Error	SE	$\times$
2	IT3_P	File_already_exist	SE	$\times$
2	IT3	File_already_exist	SE	$\times$

mining packages. More sophisticated techniques, such as feature engineering, may complement invariant-based analysis. However improving performance through ad hoc fine-tuning of algorithms for the specific dataset at hand is not within the perspective of this study, and it might have made the results tailored on the chosen datasets. We are confident that the details provided support the replication of our study by researchers and practitioners.

Internal validity. We used two different datasets and six mining algorithms to provide evidence of the actual relationships among the variables under assessment, such as number of invariants, coverage and information retrieval metrics. The use of a mixture of diverse datasets and techniques mitigates internal validity threats. The key findings of the study are consistent across the datasets and techniques, which provides a reasonable level of confidence on the analysis.

External validity. The steps of the analysis should be easily applicable to similar systems/datasets supporting the abstraction of *workload units* and *attributes*, such as systems performing batch work. Attributes, such as computing resources, duration, priority and return codes of jobs/tasks, are collectable by many established monitoring tools or available through systems/applications logs. For example, the simplest and most common way to extract attributes from logs is to *grep* the messages tracking performance and usage statistics [40]. Once mined, actionable invariants can be implemented through regular expressions to monitor production logs. Given the wide spread of log management tools, invariant mining and related applications are reasonably feasible in practice. The overhead entails the time required to establish the message types of the log that contain the metrics of interest; this is done once at the beginning of the analysis. Maybe more important, invariant-based analysis does not interfere with the system operations; features extraction, invariants mining and application can be entirely automated. Our findings, supported by measurements on real data, are useful to get an overall understanding of the characterization that can be performed through invariants and its practicability and limitations in real-world systems. We provided a number of practical suggestions in order to support the generalization of the analysis to both labelled and unlabeled datasets.

Conclusion validity. Conclusions have been inferred by assessing the sensitivity of the results with respect to the experimental choices. We assessed the sensitivity of the categories with respect to the selection of the ranges in the Google dataset: analysis indicates that the categories are not biased by the specific selection of the ranges adopted in the paper. We replicated the analysis under different configurations of key parameters, i.e., number of clusters and support. We assessed the sensitivity of the evaluation metrics with respect to the setting of the underlying mining algorithm: comparisons have been made across the optimal set of invariants in order to ensure the findings have been not biased by a particular configuration. Inferences made for the Google cluster are consistent with those of other cited studies on the same dataset. The validity of the invariant analysis for the SaaS dataset involved direct communication with the cloud operations team, which confirmed the anomalies went otherwise unnoticed.

9 Conclusions

Likely system invariants can be mined for a variety of service computing systems, including cloud systems, web service infrastructures, datacenters, enterprise systems, IT services and utility computing systems, network services, distributed systems. They represent operational abstractions of normal system dynamics. The identification and the analysis of their violations support a range of operational activities, such as runtime anomaly detection, post mortem troubleshooting, capacity planning. In this work we have used two real-world datasets - the publicly available Google datacenter dataset and a dataset of a commercial SaaS utility computing platform - for assessing and comparing three techniques for invariant mining. Analysis and comparison was based on the common metrics coverage, recall and precision.

The results provide insights into advantages and limitations of each technique, and practical suggestions to practitioners to establish the configuration of the mining algorithms and to select the number of invariants. The high-level findings are the following. A relatively small number of invariants allows to reach a relatively high coverage, i.e. they characterize the majority of executions. A small increase of the coverage of correct executions may produce a significant drop of recall and precision. The techniques exhibit similar precision, but the decision list supervised technique outperforms the unsupervised ones in recall. Finally, we presented a general heuristic for selecting a set of likely invariants from a dataset. All these results aim to fill the gap between past scientific studies and the concrete usage of likely system invariants by operations engineers.

Acknowledgments

The work by A. Pecchia and S. Russo has been supported by the GAUSS national research project (CUP E52F16002700001), funded by MIUR under the PRIN 2015 program.

The work by S. Sarkar has been initially carried out at Infosys Labs, India. His later work at BITS Pilani has been partially supported by a research grant from Accenture Technology Labs, USA.

REFERENCES

[1] M. D. Ernst, J. Cockrell, W. G. Griswold, and D. Notkin, "Dynamically Discovering Likely Program Invariants to Support Program Evolution," *IEEE Trans. on Software Engineering*, vol. 27, pp. 99–123, 2001.

[2] C. Pacheco and M. D. Ernst, "Eclat: Automatic Generation and Classification of Test Inputs," in *Proc. 19th European Conference on Object-Oriented Programming (ECOOP)*, pp. 504–527, Springer, 2005.

[3] C. Csallner and Y. Smaragdakis, "Dynamically discovering likely interface specifications," in *Proc. 28th Int. Conference on Software Engineering (ICSE)*, pp. 861–864, ACM, 2006.

[4] L. Mariani, S. Papagiannakis, and M. Pezzè, "Compatibility and regression testing of COTS-component-based software," in *Proc. 29th Int. Conference on Software Engineering (ICSE)*, ACM, 2007.

[5] J. Cobb, J. A. Jones, G. M. Kapfhammer, and M. J. Harrold, "Dynamic Invariant Detection for Relational Databases," in *Proc. 9th Int. Workshop on Dynamic Analysis*, pp. 12–17, ACM, 2011.

[6] G. Jiang, H. Chen, and K. Yoshihira, "Discovering likely invariants of distributed transaction systems for autonomic system management," *Cluster Computing*, vol. 9, pp. 385–399, 2006.

[7] H. Chen, H. Cheng, G. Jiang, and K. Yoshihira, "Invariants Based Failure Diagnosis in Distributed Computing Systems," in *Proc. 29th IEEE Int. Symp. on Reliable Distributed System (SRDS)*, pp. 160–166, IEEE, 2010.

[8] A. B. Sharma, H. Chen, M. Ding, K. Yoshihira, and G. Jiang, "Fault detection and localization in distributed systems using invariant relationships," in *Proc. 43rd IEEE/IFIP Int. Conference on Dependable Systems and Networks (DSN)*, pp. 1–8, IEEE, 2013.

[9] J.-G. Lou, Q. Fu, S. Yang, Y. Xu, and J. Li, "Mining invariants from console logs for system problem detection," in *Proc. USENIX ATC*, 2010.

[10] X. Miao, K. Liu, Y. He, D. Papadias, Q. Ma, and Y. Liu, "Agnostic diagnosis: Discovering silent failures in wireless sensor networks," *IEEE Trans. on Wireless Communications*, vol. 12, no. 12, pp. 6067–6075, 2013.

[11] S. Sarkar, R. Ganesan, M. Cinque, F. Frattini, S. Russo, and A. Savignano, "Mining Invariants from SaaS Application Logs," in *Proc. 10th European Dependable Computing Conference (EDCC)*, pp. 50–57, IEEE, 2014.

[12] G. Jiang, H. Chen, and K. Yoshihira, "Modeling and Tracking of Transaction Flow Dynamics for Fault Detection in Complex Systems," *IEEE Trans. on Dependable and Secure Computing*, vol. 3, no. 4, pp. 312–326, 2006.

[13] L. Ljung, *System Identification - Theory for The User*. Upper Saddle River, NJ, USA: Prentice Hall PTR, 2nd ed., 1998.

[14] G. Jiang, H. Chen, and K. Yoshihira, "Efficient and scalable algorithms for inferring likely invariants in distributed systems," *IEEE Trans. on Data and Knowledge Engineering*, vol. 19, pp. 1508–1523, 2007.

[15] H. Chen, H. Cheng, G. Jiang, and K. Yoshihira, "Exploiting Local and Global Invariants for the Management of Large Scale Information Systems," in *Proc. 8th IEEE Int. Conference on Data Mining (ICDM)*, pp. 113–122, IEEE, 2008.

[16] F. Frattini, S. Sarkar, J. Khasnabish, and S. Russo, "Using Invariants for Anomaly Detection: The Case Study of a SaaS Application," in *Proc. 25th Int. Symp. on Software Reliability Engineering Workshops (ISSREW)*, pp. 383–388, IEEE, 2014.

[17] C. Reiss, J. Wilkes, and J. L. Hellerstein, "Google cluster-usage traces: format + schema." http://code.google.com/p/googleclusterdata/wiki/ClusterData2011_, Nov 2011.

[18] S. Di, D. Kondo, and F. Cappello, "Characterizing Cloud Applications on a Google Data Center," in *Proc. 42nd Int. Conference on Parallel Processing (ICPP)*, pp. 468–473, IEEE, 2013.

[19] X. Chen, C.-D. Lu, and K. Pattabiraman, "Failure Analysis of Jobs in Compute Clouds: A Google Cluster Case Study," in *Proc. 25th Int. Symp. on Software Reliability Engineering (ISSRE)*, pp. 167–177, IEEE, 2014.

[20] X. Chen, C.-D. Lu, and K. Pattabiraman, "Failure Prediction of Jobs in Compute Clouds: A Google Cluster Case Study," in *Proc. 25th Int. Symp. on Software Reliability Engineering Workshops (ISSREW)*, pp. 341–346, IEEE, 2014.

[21] Q. Guan and S. Fu, "Adaptive anomaly identification by exploring metric subspace in cloud computing infrastructures," in *Proc. 32nd Int. Symp. on Reliable Distributed Systems (SRDS)*, pp. 205–214, IEEE, 2013.

[22] A. Rosà, L. Y. Chen, and W. Binder, "Failure analysis and prediction for big-data systems," *IEEE Trans. on Services Computing*, 2016.

[23] V. Chudnovsky, R. Rifaat, J. Hellerstein, B. Sharma, and C. Das, "Modeling and synthesizing task placement constraints in google compute clusters," in *Proc. 2nd ACM Symp. on Cloud Computing*, ACM, 2011.

[24] C. Di Martino, Z. Kalbarczyk, R. K. Iyer, G. Goel, S. Sarkar, and R. Ganesan, "Characterization of operational failures from a business data processing SaaS platform," in *Proc. 36th Int. Conference on Software Engineering (ICSE)*, pp. 195–204, ACM, 2014.

[25] V. Chandola, A. Banerjee, and V. Kumar, "Anomaly detection: A survey," *ACM Computing Surveys*, vol. 41, no. 3, pp. 15:1–15:58, 2009.

[26] Z. Ren, J. Wan, W. Shi, X. Xu, and M. Zhou, "Workload analysis, implications, and optimization on a production hadoop cluster: A case study on taobao," *IEEE Trans. on Services Computing*, vol. 7, no. 2, pp. 307–321, 2014.

[27] R. Jain, *The Art of Computer Systems Performance Analysis*. John Wiley & Sons New York, 1991.

[28] P. Garraghan, I. Solis, Moreno, P. Townend, and J. Xu, "An Analysis of Failure-Related Energy Waste in a Large-Scale Cloud Environment," *IEEE Trans. on Emerging Topics in Computing*, vol. 2, no. 2, pp. 166–180, 2014.

[29] I. Guyon and A. Elisseeff, "An introduction to variable and feature selection," *J. Mach. Learn. Res.*, vol. 3, pp. 1157–1182, Mar. 2003.

[30] R. Xu and D. Wunsch, *Clustering*. Wiley-IEEE Press, 2009.

[31] M. Ester, H.-P. Kriegel, J. Sander, and X. Xu, "A density-based algorithm for discovering clusters in large spatial databases with noise," in *Proc. 2nd Int. Conference on Knowledge Discovery and Data Mining*, KDD'96, pp. 226–231, AAAI Press, 1996.

[32] S. Brin, R. Motwani, J. D. Ullman, and S. Tsur, "Dynamic itemset counting and implication rules for market basket data," *ACM SIGMOD Rec.*, vol. 26, no. 2, pp. 255–264, 1997.

[33] R. Agrawal and R. Srikant, "Fast algorithms for mining association rules in large databases," in *Proc. 20th Int. Conference on Very Large Data Bases (VLDB)*, pp. 487–499, Morgan Kaufmann, 1994.

[34] R. Srikant and R. Agrawal, "Mining sequential patterns: Generalizations and performance improvements," in *Proc. 5th Int. Conference on Extending Database Technology: Advances in Database Technology (EDBT)*, pp. 3–17, Springer-Verlag, 1996.

[35] C. Borgelt and R. Kruse, "Induction of Association Rules: Apriori Implementation," in *Compstat - Proceedings in Computational Statistics* (W. Härdle and B. Rönz, eds.), pp. 395–400, Physica-Verlag, 2002.

[36] E. Frank and I. H. Witten, "Generating accurate rule sets without global optimization," in *Proc. 15th Int. Conference on Machine Learning (ICML)*, pp. 144–151, Morgan Kaufmann, 1998.

[37] M. Hall and E. Frank, "Combining naive bayes and decision tables," in *Proc. 21st Florida Artificial Intelligence Society Conference (FLAIRS)*, pp. 318–319, AAAI press, 2008.

[38] R. O. Duda and P. E. Hart, *Pattern classification and scene analysis*. J. Wiley and Sons, 1973.

[39] C. Wohlin, P. Runeson, M. Höst, M. C. Ohlsson, B. Regnell, and A. Wesslén, *Experimentation in Software Engineering: An Introduction*. Kluwer Academic, 2000.

[40] A. Oliner, A. Ganapathi, and W. Xu, "Advances and challenges in log analysis," *Commun. ACM*, vol. 55, pp. 55–61, Feb. 2012.

Antonio Pecchia received the B.S. (2005), M.S. (2008) and Ph.D. (2011) in Computer Engineering from the Federico II University of Naples, where he is lecturer in Advanced Computer Programming. He is a post-doc at CINI in European projects, and co-founder of the Critiware spin-off company (www.critiware.com). His research interests include data analytics, log-based failure analysis, dependable and secure distributed systems.

Stefano Russo is Professor of Computer Engineering at the Federico II University of Naples, where he teaches Software Engineering and Distributed Systems, and leads the DEpendable Systems and Software Engineering Research Team (DESSERT, www.dessert.unina.it). He co-authored over 160 papers in the areas of software engineering, middleware technologies, mobile computing. He is Senior Member of IEEE.

Santonu Sarkar received the PhD in computer science from the Indian Institute of Technology, Kharagpur. He is professor of computer science and information systems at BITS Pilani, K.K.Birla Goa Campus. He has more than 20 years of experience in IT industry in applied research, product development, project and client account management. His current research interests include software engineering techniques to ensure dependability, performance, and ease-of-use of Cloud and HPC applications. Prior to this, he had worked in the areas of software metrics and measurement, software design and architectures, program comprehension, reengineering techniques.